

Fault Detection and Isolation of a Polyethylene Reactor Using Asynchronous Measurements

Charles W. McFall, David Muñoz de la Peña, Ben Ohran,
Panagiotis D. Christofides, and James F. Davis

Abstract—This work applies the method of fault-detection and isolation for nonlinear processes when some process variable measurements are available at regular sampling intervals and the remaining process variables are measured at an asynchronous rate to a gas-phase polyethylene reactor model. First, the fault-detection and isolation (FDI) scheme that employs model-based techniques for the isolation of faults is reviewed. The FDI scheme provides detection and isolation of any fault that enters into the differential equation of only synchronously measured states, and grouping of faults that enter into the differential equation of any asynchronously measured state. For a fully coupled process system, fault-detection occurs shortly after a fault takes place, and fault isolation, limited by the arrival of asynchronous measurements, occurs when asynchronous measurements become available. Fault-tolerant control methods with a supervisory control component are then employed to achieve stability in the presence of actuator failures using control system reconfiguration. Numerical simulations of the polyethylene reactor are performed, demonstrating the applicability and performance of the proposed fault-detection and isolation and fault-tolerant control method in the presence of asynchronous measurements.

I. INTRODUCTION

Automation is a key component to the operation of any modern chemical process because it helps deal with environmental, safety, and economic concerns in real time. Increased levels of automation, however, may leave a chemical process vulnerable to failures such as actuator faults, sensor errors, or controller faults that may lead to waste of energy or feedstock, and in some cases environmental and/or safety problems. At least 10 billion USD are lost annually in the US due to abnormal situations in chemical and process industries [1], thus, timely detection and isolation and efficient handling of these situations is of critical importance. This work addresses the issue of handling abnormal situations considering that process measurements used for feedback control and process monitoring are typically asynchronous. This can be due to the nature of the measurement itself (i.e., concentration measurements may be difficult to obtain while temperature measurements are usually readily available) or due to the use of sensor networks (wired or wireless) that

C. W. McFall, B. J. Ohran, P. D. Christofides and J. F. Davis are with the Department of Chemical and Biomolecular Engineering, University of California, Los Angeles, CA 90095-1592, USA. P. D. Christofides is also with the Department of Electrical Engineering, University of California, Los Angeles, CA 90095-1592, USA. D. Muñoz de la Peña is with Departamento de Ingeniería de Sistemas y Automática, Universidad de Sevilla, Camino de los Descubrimientos S/N, 41092, Sevilla, Spain. Corresponding author: P. D. Christofides, Email: pdc@seas.ucla.edu.

may introduce complex dynamics into the monitoring system due to field interference.

The first component required to develop a control scheme that is robust to failures is an automatic fault-detection and isolation (FDI) scheme that will find the source of failures in a timely manner. Recently, research has been done on the topic of feedback control with asynchronous measurements [2], [3]. These efforts provide a starting framework for control subject to asynchronous measurements, but they do not include FDI. The goal of this work is to demonstrate the application of an FDI scheme that will allow fault tolerant control (FTC) to take place when process measurements are available at asynchronous time instants. First, an FDI scheme that employs model-based techniques is reviewed that allows for the isolation of faults. This scheme employs model-based FDI filters similar to those found in [4] in addition to observers that estimate the fault free evolution of asynchronously measured states during time intervals in which their measurements are not available. Specifically, the FDI scheme provides detection and isolation of any fault that enters into the differential equation of only synchronously measured states, and grouping of faults that enter into the differential equation of any asynchronously measured state. For a fully coupled process system, fault-detection occurs shortly after a fault takes place, and fault isolation, limited by the arrival of asynchronous measurements, occurs when asynchronous measurements become available. Once the FDI methodology has provided the system supervisor with a fault diagnosis, the supervisor takes appropriate action to seamlessly reconfigure the system to an alternative control configuration that will enforce the desired operation. This work applies this asynchronous FDI and FTC framework to a polyethylene reactor simulation [5].

II. FDI USING ASYNCHRONOUS MEASUREMENTS: PROBLEM FORMULATION AND SOLUTION

A. Class of nonlinear systems

In this work, we consider nonlinear process systems described by the following state-space model

$$\begin{aligned}\dot{x}_s &= f_s(x_s, x_a, u, d) \\ \dot{x}_a &= f_a(x_s, x_a, u, d)\end{aligned}\quad (1)$$

where $x_s \in R^{n_s}$ denotes the set of state variables that are sampled synchronously, $x_a \in R^{n_a}$ denotes the set of state variables that are sampled asynchronously, $u \in R^{n_u}$ denotes the input and $d \in R^p$ is a model of the set of p possible

faults. The faults are unknown and $d_j, j = 1 \dots p$, can take any value. The state of the full system is given by the vector

$$x = \begin{bmatrix} x_s \\ x_a \end{bmatrix} \in R^{n_s+n_a}$$

Using this definition for x , the system of Eq.1 can be written in the following equivalent compact form

$$\dot{x} = f(x, u, d) \quad (2)$$

We assume that f is a locally Lipschitz vector function and that $f(0, 0, 0) = 0$. This means that the origin is an equilibrium point for the fault-free system with $u(t) \equiv 0$. Moreover, we assume that the fault-free system ($d_i(t) \equiv 0$ for all t) has an asymptotically stable equilibrium at the origin $x = 0$ for a given feedback control function $h : R^{n_s+n_a} \rightarrow R^{n_u}$ which satisfies $h(0) = 0$.

B. Modeling of asynchronous measurements

The system of Eq.1 is controlled using both sampled synchronous and asynchronous measurements. We assume that each state $x_{s,i}, i = 1 \dots n_s$ is sampled continuously (i.e., at intervals of fixed size $\Delta > 0$ where Δ is a sufficiently small positive number). Each state $x_{a,i}, i = n_s + 1 \dots n_s + n_a$, is sampled asynchronously and is only available at time instants $t_{k,i}$ where $t_{k,i}$ is a random increasing sequence of times. A controller design that takes advantage of the asynchronous measurements must take into account that it will have to operate without complete state information between asynchronous samples. This class of systems arises naturally in process control, where process variables such as temperature, flow, or concentration have to be measured. In such a case, temperature and flow measurements can be assumed to be available continuously. Concentration measurements, however, are available at an asynchronous sampling rate.

If there exists a non-zero probability that the system operates in open-loop for a period of time large enough for the state to leave the stability region or even diverge to infinity (i.e., finite escape time), it is not possible to provide guaranteed stability properties. In order to study the stability properties in a deterministic framework, we consider systems where there is a limit on the maximum number of consecutive sampling times in which measurements of $x_{a,i}$ are not available, i.e.

$$\max(t_{k,i} - t_{k+1,i}) \leq \Delta_M$$

This bound on the maximum period of time in which the loop is open has been also used in other works in the literature [6], [7], [2] and allows us to study deterministic notions of stability.

C. Asynchronous state observer

An observer that takes advantage of both synchronous and asynchronous measurements can be constructed to estimate the fault-free evolution of asynchronous states between consecutive measurements. The observer states are updated by setting the observer state equal to the measurement each time

a new asynchronous measurement becomes available at $t_{k,i}$. The asynchronous state observer takes the form

$$\dot{\hat{x}}_a = f_a(x_s, \hat{x}_a, u, 0) \quad (3)$$

with $\hat{x}_{a,i}(t_{k,i}) = x_{a,i}(t_{k,i})$ for all $t_{k,i}$; that is, each time a new asynchronous measurement is received, the estimated states $\hat{x}_{a,i}$ with $i = n_s + 1, \dots, n_s + n_a$ are reset to match the true process state. The information generated by this observer provides a fault-free estimate for each asynchronous state at any time t and allows for the design of non-linear control laws that utilize full state information. Using the estimated states, the control input applied to the system is given by $u = h(\hat{x})$ where $\hat{x} = [x_s^T \hat{x}_a^T]^T$.

This control input is defined for all times because it is based on both the synchronous states and the estimated asynchronous states. We assume that Δ_M is small enough to guarantee that the system in closed-loop with this control scheme is practically stable, see [6], [7], [2] for details on similar stability results.

D. Design of fault-detection and isolation filter

In this section we construct fault-detection and isolation (FDI) filters that will automatically identify the source of a failure in a timely manner. Utilizing both synchronous state measurements, $\hat{x}_i(t), i = 1 \dots n_s$, and asynchronous state estimates, $\hat{x}_i(t), i = n_s + 1 \dots n_s + n_a$, the following $n_s + n_a$ filters are defined [4]:

$$\dot{\tilde{x}}_i = f_i(\hat{x}_1 \dots \tilde{x}_i \dots \hat{x}_{n_s+n_a}, h(\hat{x}_1 \dots \tilde{x}_i \dots \hat{x}_{n_s+n_a}), 0) \quad (4)$$

where \tilde{x}_i is the filter output for the i^{th} state in \hat{x} and f_i is the i^{th} component of the vector function f . The FDI filters are only initialized at $t = 0$ such that $\tilde{x}(0) = \hat{x}(0)$. For each state in \hat{x} , the FDI residual can be defined as

$$r_i(t) = |\hat{x}_i(t) - \tilde{x}_i(t)|, i = 1 \dots, n_s + n_a.$$

The synchronous residuals $r_i(t)$ with $i = 1, \dots, n_s$ are computed continuously because $\hat{x}_i(t)$ with $i = 1, \dots, n_s$ is known for all t . On the other hand, the asynchronous residuals $r_i(t), i = n_s + 1 \dots n_s + n_a$, are computed only at times $t_{k,i}$ when a new asynchronous measurement of $\hat{x}_i(t), i = n_s + 1 \dots n_s + n_a$, is received. These FDI filters operate by essentially predicting the fault-free evolution of each individual state, accounting for faults that enter the system when the predicted evolution of the state diverges from the measured evolution [4].

The dynamics of the synchronous states and asynchronous observers, \hat{x} , and the FDI filters, \tilde{x}_i , are identical to those of the system of Eq.1 when there are no disturbances or noise acting on the system. When the states are initialized as $\hat{x}(0) = \tilde{x}(0) = x(0)$ both the observer and filter states will track the true process states. For faults affecting the synchronous states, when a fault, d_j , occurs, only the residual corresponding to the affected state, r_i , will become nonzero. This is the case when the $f_s(x_s, x_a, h(x), d)$ vector field has a structure such that type I faults are isolable; see [4] for a precise determination of such a structure. In the case

with faults affecting asynchronously measured states, at least one r_i will become non-zero when a fault occurs. However, faults that affect asynchronous states cause the asynchronous observer \hat{x}_a to diverge from the true process state x_a between consecutive measurements, and any FDI filter states that are a function of \hat{x}_a will no longer accurately track the corresponding true process states. When such a fault occurs more than one residual value may become nonzero.

Continuous measurements for asynchronous states are not available, thus the FDI filters in Eq.4 cannot always completely isolate all failures. We consider two classes of faults. Type I faults are faults that only affect states that are measured continuously; that is, d_j is a type I fault if

$$\frac{\partial f_i}{\partial d_j} = 0, \forall i = n_s + 1, \dots, n_s + n_a.$$

Type II faults affect at least one asynchronous state; that is, d_j is a type II fault if there exists at least one $i = n_s + 1, \dots, n_s + n_a$ such that

$$\frac{\partial f_i}{\partial d_j} \neq 0.$$

The FDI filter will detect and isolate a type I fault d_j because the asynchronous state observers will track the asynchronous states accurately (i.e., the effect of the fault $d_j(t)$ on an asynchronous observer state is accounted for through the synchronous states, so $d_j(t)$ is accounted for in the observer of Eq.3 and hence the FDI filter). A type II fault enters the system in the differential equation of a state that is sampled asynchronously. The effect of type II faults cannot be accounted for by the observer \hat{x}_i , and such a fault will cause \hat{x}_i to no longer track x_i and will eventually affect other coupled filter states as well. Strict isolation cannot take place for a type II fault. The FDI filter will detect and partially isolate disturbances in this case because the asynchronous state observers will diverge from the asynchronous states (i.e., the effect of the fault $d_j(t)$ on an asynchronous observer state is unmeasured and unaccounted for, thus the observer in Eq.3 does not track the disturbed state). In other words, if a type I fault occurs, then it can be detected and isolated. If a type II fault occurs, then this fault can be grouped to the subset of type II faults.

A fault is detected at time t_f if there exists a residual i such that $r_i(t_f) > r_{i,max}$, where $r_{i,max}$ is an appropriate threshold chosen to account for process and sensor noise. In order to isolate the possible source of the fault, it is necessary to wait until the residuals of all the asynchronous state filters are updated after t_f to determine if the fault is type I or type II. The residual of each asynchronous state filter \tilde{x}_i is updated at time

$$t_i(t_f) = \min_k t_{k,i} | t_{k,i} > t_f.$$

If $r_i(t_i(t_f)) \leq r_{i,max}$ with $i = n_s + 1, \dots, n_s + n_a$, then the fault occurred at time t_f is a type I fault and can be appropriately isolated. Otherwise, the fault belongs to the set of type II faults.

Consider that a synchronous residual r_i indicates a fault at time t_f . In this case the fault could have two possible

causes, a type I or type II fault. In order to determine the true cause of this fault, one has to wait for the complete set of asynchronous measurements to arrive after t_f . When all the asynchronous measurements arrive and if all the residuals of the asynchronous states are smaller than the threshold, then the fault can be attributed to a type I fault. If any asynchronous measurement arrives and the corresponding residual indicates a fault, then the fault is type II. Note that when an asynchronous residual indicates a fault, we can also conclude that the fault is type II. When the fault is type II it has been detected, and it is possible to narrow the fault source down to the set of faults that enter the differential equations of asynchronous states.

When the fault can be attributed to a type I fault and it has been detected and isolated, then automated fault tolerant (FTC) control action can be initiated. For example, when a fault event that is due to a manipulated input failure (i.e., an actuator failure) is detected and isolated, fault tolerant control methods can be initiated [4]. In general an FTC switching rule may be employed that orchestrates the re-configuration of the control system in the event of control system failure. This rule determines which of the backup control loops can be activated, in the event that the main control loop fails, in order to preserve closed-loop stability. Owing to the limitations imposed by input constraints on the stability region for each control configuration, switching from a malfunctioning configuration to a well-functioning, but randomly selected, backup configuration will not preserve closed-loop stability if the state of the system, at the time of failure, lies outside the stability region of the chosen backup configuration. In this case, stabilization using this configuration requires more control action than is allowed by its constraints. This observation motivates the development of switching logic, which is to switch to the control configuration for which the closed-loop state resides within the stability region at the time of control failure. Without loss of generality, let the initial actuator configuration be $k(0) = 1$ and let t_d be the time when this failure has been isolated, then the switching rule given by

$$k(t) = j \quad \forall t \geq t_d \text{ if } x(t_d) \in \Omega(u_j^{max}) \quad (5)$$

for some $j \in \{2, 3, \dots, N\}$ guarantees closed-loop asymptotic stability, where $\Omega(u_j^{max})$ is the stability region for the j^{th} control configuration. The implementation of the above switching law requires monitoring the closed-loop state trajectory with respect to the stability regions associated with the various fall-back configurations. The reader may refer to [8] for application of FTC to a polyethylene reactor with constraints on the manipulated inputs. In this work we consider a control law without constraints on the manipulated inputs, and the primary control configuration with a faulty actuator will be deactivated in favor of a fully functional fall-back control configuration where the fall-back configuration can guarantee global stability of the closed-loop system. This integrated FDI/FTC reconfiguration allows for seamless fault-recovery in the event of an actuator failure. Section III demonstrates integrated FDI/FTC for the polyethylene reactor.

III. APPLICATION TO A POLYETHYLENE REACTOR WITH ASYNCHRONOUS MEASUREMENTS

A. Process and measurement modeling

The proposed model-based asynchronous FDI and FTC method will be demonstrated using a model of an industrial gas phase polyethylene reactor. The feed to the reactor consists of ethylene ($[M_1]$), comonomer, hydrogen, inerts ($[In]$) and catalyst (Y). A recycle stream of unreacted gases flows from the top of the reactor and is cooled by passing through a water-cooled heat exchanger. Cooling rates in the heat exchanger are adjusted by mixing cold and warm water streams while maintaining a constant total cooling water flow rate through the heat exchanger. Mass balances on hydrogen and comonomer have not been considered in this study because hydrogen and comonomer have only mild effects on the reactor dynamics [5]. A mathematical model for this reactor can be found in [9]. We do not list the dynamic equations here for brevity, but the model and parameters used matches that in [9] and can also be found in the submitted full version of this paper [10]. Under normal operating conditions, the open-loop system behaves in an oscillatory fashion (i.e., the system possesses an open-loop unstable steady-state surrounded by a stable limit cycle). The open-loop unstable steady-state around which the system will be controlled is

$$\begin{aligned} [In]_{ss} &= 439.7 \frac{mol}{m^3} & [M_1]_{ss} &= 326.7 \frac{mol}{m^3} \\ Y_{ss} &= 7.67 mol & T_{ss} &= 356.2 K \\ T_{g1ss} &= 290.4 K & T_{w1ss} &= 294.4 K. \end{aligned}$$

where T , T_{g1} and T_{w1} are the temperatures of the reactor, recycle gas after cooling and exit-stream cooling water, respectively. In this example, we consider four possible faults, d_1, d_2, d_3 , and d_4 which represent a heat jacket fault, catalyst deactivation, a change in the recycle gas flow rate, and ethylene consumption, respectively. The primary manipulated input for these studies is the heat input, Q , and the fall-back manipulated input is the feed temperature, T_{feed} . A fall-back manipulated input is required to maintain desired system performance in the presence of failure in the primary control configuration.

Simulations have been carried out for several scenarios to demonstrate the effectiveness of the proposed FDI scheme in detecting and isolating the four faults d_1, d_2, d_3 , and d_4 in the presence of asynchronous measurements. The temperature measurements (T, T_{g1}, T_{w1}) are all assumed to be available synchronously, while the concentration measurements ($[In], [M_1], Y$) arrive at asynchronous intervals. In all the simulations, sensor measurement and process noise are included. The sensor measurement noise trajectory was generated using a sample time of ten seconds and a zero-mean normal distribution with standard deviation σ_M . The autoregressive process noise was generated discretely as $w_k = \phi w_{k-1} + \xi_k$ where $k = 0, 1, \dots$ is the discrete time step, with a sample time of ten seconds, ϕ is the autoregressive coefficient and ξ_k is obtained at each sampling step using a zero-mean normal distribution with standard

TABLE I
POLYETHYLENE REACTOR NOISE PARAMETERS

	σ_p	σ_m	ϕ
$[In]$	1E-4	5E-2	0
$[M_1]$	1E-4	5E-2	0.7
Y	1E-4	1E-2	0.7
T	5E-3	5E-2	0.7
T_{g1}	5E-3	5E-2	0.7
T_{w1}	5E-3	5E-2	0.7

deviation σ_p . The autoregressive process noise is added to the right-hand side of the differential equations for each state and the sensor measurement noise is added to the measurements of each state. Sensor measurement noise and process noise are evaluated independently for each state variable. Table I provides the values of the noise parameters for each state of the system. The length of time between consecutive asynchronous measurements is generated randomly based on a Poisson process. The time when the system will receive the next asynchronous measurement of the i^{th} state is given by $t_{k+1,i} = t_{k,i} + \Delta_a$ where $\Delta_a = -\ln(\xi)/W_a$ and $\xi \in (0, 1)$ is a random variable chosen from a uniform probability distribution and $W_a = 0.003 \text{ s}^{-1}$ is the mean rate of asynchronous sampling. There is an upper bound limiting the time between consecutive measurements such that $\Delta_a \leq \Delta_M = 1200 \text{ s}$. This value of Δ_M is small enough to provide practical closed-loop stability around the desired equilibrium point for the polyethylene reactor. An increasing sequence of measurement arrival times is generated independently for each asynchronously measured state.

B. Design of the asynchronous state observers

To perform FDI for the polyethylene reactor system we need to construct the asynchronous state observers of the form in Eq.3, where $[\hat{In}]$, $[\hat{M}_1]$, and \hat{Y} are the asynchronous observer states. Each asynchronous observer state is initialized each time new measurement information becomes available at the times $t_{k,i}$. The observer states provide estimates for the asynchronous states between consecutive measurements allowing the computation of control actions and FDI residuals at each time.

C. Design of the state feedback controller

The control objective is to stabilize the system at the open-loop unstable steady state. A nonlinear Lyapunov-based feedback controller that enforces asymptotic stability of the closed-loop system is synthesized using the method proposed in [11] (see also [12]). This is a single input controller that utilizes synchronous measurements as well as observer states. The polyethylene reactor dynamics belong to the following class of non-linear systems

$$\dot{x}(t) = f(x(t)) + g_1(x(t))u_1(t) + g_2(x(t))u_2(t) + w(x(t))d(t) \quad (6)$$

where

$$x(t) = \begin{bmatrix} [In] - [In]_{ss} \\ [M_1] - [M_1]_{ss} \\ Y - Y_{ss} \\ T - T_{ss} \\ T_{g1} - T_{g1ss} \\ T_{w1} - T_{w1ss} \end{bmatrix}$$

and

$$u_1(t) = Q, \quad u_2(t) = T_{feed}.$$

Consider the quadratic control Lyapunov function $V(x) = x^T P x$ where

$$P = 1 \times 10^{-2} \text{diag}[0.5 \ 0.5 \ 0.5 \ 1 \ 0.005 \ 0.005].$$

The values of the weighting matrix P are chosen to account for the different range of numerical values for each state. The following feedback laws [11] asymptotically stabilize the open-loop and possibly unstable steady-state of the nominal system (i.e., $d(t) \equiv 0$)

$$h_i(x) = \begin{cases} \frac{L_f V + \sqrt{L_f V^2 + L_{g_i} V^4}}{-L_{g_i} V} & \text{if } L_{g_i} V \neq 0 \\ 0 & \text{if } L_{g_i} V = 0 \end{cases}, \quad i = 1, 2. \quad (7)$$

where $L_f V$ and $L_{g_i} V$ denote the Lie derivatives of the scalar function V with respect to the vectors fields f and g_i respectively.

In the simulations, the primary control configuration is given by

$$u_1(t) = h_1(\hat{x}(t))$$

and the fall-back control configuration is given by

$$u_2(t) = h_2(\hat{x}(t))$$

where

$$\hat{x}(t) = \begin{bmatrix} [\hat{In}] - [In]_{ss} \\ [\hat{M}_1] - [M_1]_{ss} \\ \hat{Y} - Y_{ss} \\ T - T_{ss} \\ T_{g1} - T_{g1ss} \\ T_{w1} - T_{w1ss} \end{bmatrix}.$$

D. Design of FDI/FTC scheme

Fault-detection and isolation for the system in closed-loop with the primary configuration is accomplished by generating FDI filters as in Eq.4. In addition, the FDI residuals take the following form:

$$\begin{aligned} r_{[In]} &= |[\hat{In}](t_k) - [\tilde{In}](t_k)| \\ r_{[M_1]} &= |[\hat{M}_1](t_k) - [\tilde{M}_1](t_k)| \\ r_Y &= |\hat{Y}(t_k) - \tilde{Y}(t_k)| \\ r_T &= |T - \tilde{T}| \\ r_{T_{g1}} &= |T_{g1} - \tilde{T}_{g1}| \\ r_{T_{w1}} &= |T_{w1} - \tilde{T}_{w1}|. \end{aligned} \quad (8)$$

In the case with measurement and process noise, the residuals will be nonzero even without a failure event. This motivates the use of detection thresholds such that a fault is declared when a residual exceeds a specific threshold value, $r_{i,max}$

(note that a different threshold value can be used for each residual, see Remark 2). This threshold value must be selected to avoid false alarms due to process and measurement noise, but it should also be sensitive enough (small enough) to detect faults in a timely manner so that efficient FTC action can be initiated. The threshold values used for each residual in the numerical simulations can be seen as the dashed lines in Figures 3, 5, 7, and 9.

If the fault can be isolated to d_1 (i.e., r_T exceeds $r_{T,max}$ at $t = t_f$, while $r_i(t_i(t_f)) \leq r_{i,max}$ with $i = [In], [M_1], Y$), then one can invoke fault tolerant control methods to handle actuator failures by activation of a fall-back control configuration. In the simulation studies, it is assumed that a fall-back configuration, where the fall-back manipulated input $u_2 = T_{feed}$, is available. The control law of (7) enforces stability when the control actuator is functioning properly, thus switching to the operational fall-back configuration will guarantee stability in the case of failure of the primary control configuration, $u_1 = Q$.

E. Closed-loop process simulation results

This section consists of four simulation studies, each examining one of the faults d_1, d_2, d_3 , or d_4 . The first simulation considers a fault, d_1 , on the heating jacket which is the primary manipulated input. In this case the simulation includes fault tolerant control that automatically reconfigures the plant so that the fall-back manipulated input, $u_2 = T_{feed}$, is activated to maintain stability. Specifically, the supervisory control element will deactivate the primary control configuration, u_1 and activate the fall-back configuration u_2 when $r_T > r_{T,max}$ and $r_i(t_i(t_f)) \leq r_{i,max}$ with $i = [In], [M_1], Y$. This specific fault signature corresponds to a type I fault that can be isolated to d_1 . The reader may refer to [8] to obtain more information on FTC and reconfiguration rules for a polyethylene reactor with constraints on the manipulated inputs that give rise to stability regions. This work does not consider constraints on the manipulated inputs, hence, the fall-back configuration can guarantee stability from anywhere in the state space because the closed-loop system under the fall-back control configuration is globally asymptotically stable. The remaining simulation studies explore faults that disturb the system, but do not arise from actuator failures. Since they are not caused by actuation component malfunctions these failures cannot be resolved simply by actuator reconfiguration. However, these simulations demonstrate quick detection and isolation in the presence of asynchronous measurements that enables the operator to take appropriate and focused action in a timely manner.

For the fault d_1 a simulation study has been carried out to demonstrate the proposed asynchronous fault-detection and isolation and fault tolerant control method. The sequence of asynchronous measurements for this scenario is shown in Figure 1. This first simulation uses the primary control configuration in which Q is the manipulated input and has a fall-back configuration, in which T_{feed} is the manipulated input, available in case of a fault in d_1 . A fault takes place where $d_1 = 1 \text{ K/s}$ at $t = 0.5 \text{ hr}$ representing a failure in

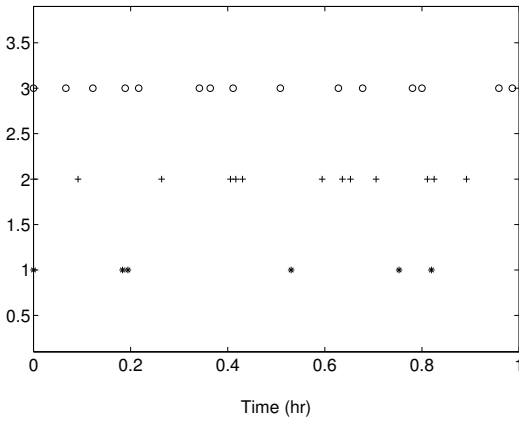


Fig. 1. Asynchronous sampling times $t_{k,[In]}$ (star), $t_{k,[M_1]}$ (cross), and $t_{k,Y}$ (circle) with a fault d_1 at $t = 0.5$ hr.

the heating jacket, Q . At this time the synchronous states in Figure 2 all move away from the equilibrium point. Additionally, as asynchronous measurements become available, it is clear the asynchronous states also move away from the equilibrium point after the failure. It is unclear from the state information alone what caused this faulty behavior. However, if the FDI residuals in Figure 3 are examined, it is clear that the residual r_T that is associated with the manipulated input Q , violates its threshold at $t_f = 0.5003$ hr. The fault is detected upon this threshold violation. However, isolation cannot take place until one new measurement for each asynchronous state becomes available. At $t = 0.5944$ hr all three required asynchronous measurements have arrived, and the asynchronous residuals remain below their thresholds, hence $r_i(t_i(t_f)) \leq r_{i,max}$ with $i = [In], [M_1], Y$. This signals that this is a type I fault that can be isolated to d_1 . At this time, the system is reconfigured to the fall-back configuration where T_{feed} is the manipulated input, and the resulting state trajectory, shown as the dotted line in Figure 2, moves back to the desired operating point. The manipulated input trajectories are not included here for brevity, but can be found in the submitted full paper [10]. The manipulated input for this scenario can be seen in Figure 4 where the solid line is the manipulated input without detection and reconfiguration, and the dotted line represents the input after FDI and reconfiguration.

The second simulation demonstrates the proposed asynchronous model-based fault-detection and isolation method when a type II fault occurs. The sequence of asynchronous measurements for this scenario are:

$$\begin{aligned} t_{k,[In]} &= [0, 0.02, 0.13, 0.17, 0.22, 0.38, 0.39, 0.47, \\ &\quad 0.50, 0.53, 0.65, 0.84, 0.98] \text{ hr} \\ t_{k,[M_1]} &= [0, 0.32, 0.55, 0.70, 0.70, 0.71, 0.83] \text{ hr} \\ t_{k,Y} &= [0, 0.02, 0.13, 0.16, 0.17, 0.22, 0.38, 0.39, \\ &\quad 0.47, 0.50, 0.53, 0.65, 0.84, 0.98] \text{ hr}. \end{aligned}$$

This simulation uses the primary control configuration in which Q is the manipulated input. A fault takes place where $d_2 = -0.001$ mol/s at $t = 0.5$ hr representing a catalyst deactivation event. After the failure, two synchronous states

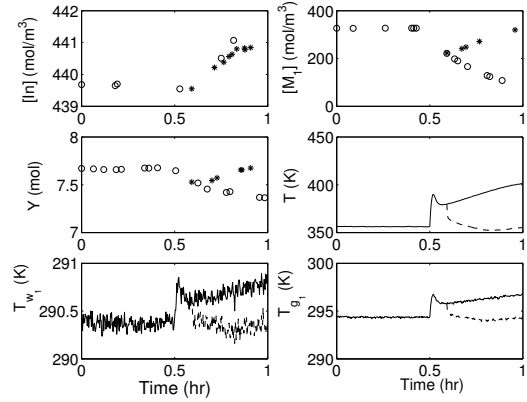


Fig. 2. State trajectories of the closed-loop system without fault-tolerant control (circle/solid) and with appropriate fault-detection and isolation and fault-tolerant control where the fall-back control configuration is activated (star/dotted) with a fault d_1 at $t = 0.5$ hr.

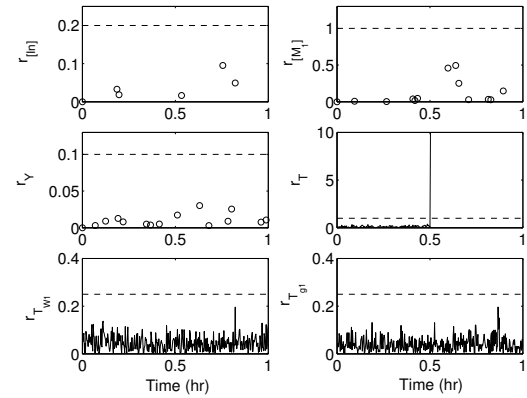


Fig. 3. Fault-detection and isolation residuals for the closed-loop system with a fault d_1 at $t = 0.5$ hr. The fault is detected immediately, but isolation occurs at $t = 0.59$ hr when all three asynchronous states have reported a residual below their detection threshold. This signals a type I fault, and we can isolate the source of this fault as d_1 .

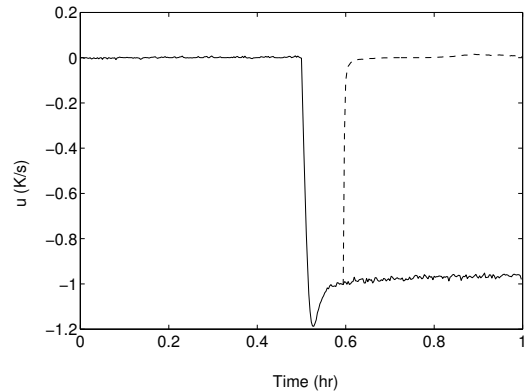


Fig. 4. Manipulated input for the closed-loop system without fault-tolerant control (solid) and with appropriate fault-tolerant control where the fall-back control configuration is activated (dotted) with a fault d_1 at $t = 0.5$ hr.

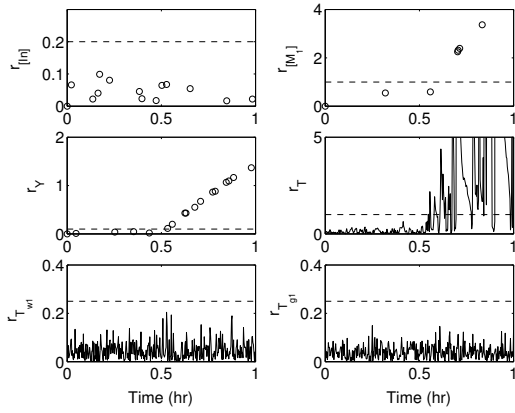


Fig. 5. Fault-detection and isolation residuals for the closed-loop system with a fault d_2 at $t = 0.5$ hr. The fault is detected when residual for Y exceeds the threshold. Subsequently, T and $[M_1]$ exceed their thresholds. When any asynchronous residual violates the threshold this indicates that the fault is in the set of type II faults; d_2 or d_4 .

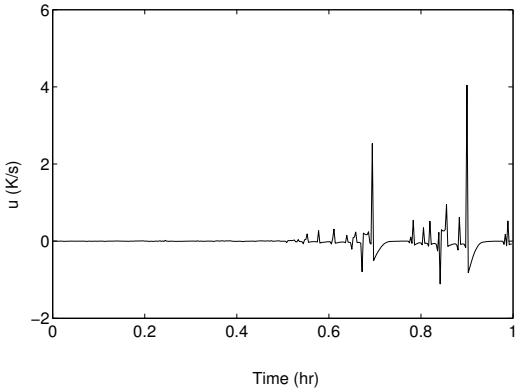


Fig. 6. Manipulated input for the closed-loop system with a fault d_2 at $t = 0.5$ hr.

in move away from the equilibrium point (see [10] for additional figures). Additionally, as asynchronous measurements become available it can be seen that asynchronous states also move away from the equilibrium point after the failure. It is unclear from the state information alone what caused this faulty behavior. However, if the FDI residuals in Figure 5 generated by (8) are examined, it is clear that the residuals $r_{[M_1]}$, r_Y , and r_T violate their thresholds. The fault is detected upon the first threshold violation (r_Y at $t = 0.5333$ hr). When the residual associated with Y exceeds the threshold this signals that the fault is type II and entered the system in the differential equation of an asynchronous state. When the fault is type II it cannot be isolated. However, such a fault can be grouped in the subset of faults that enter into the differential equation of an asynchronous state, (i.e., the group of type II faults, specifically, d_2 or d_4). At this time, the system operator can utilize the above partial isolation to examine the plant and determine the exact source of the failure. The manipulated input for this scenario can be seen in Figure 6.

The third simulation study examines FDI in the presence of a type I fault, d_3 , representing a change in the recycle gas

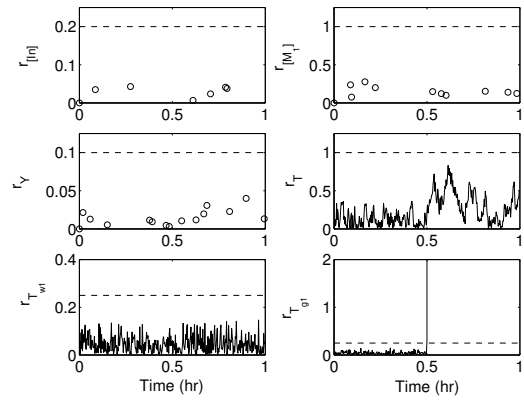


Fig. 7. Fault-detection and isolation residuals for the closed-loop system with a fault d_3 at $t = 0.5$ hr. A fault is detected immediately when residual for T_{g1} exceeds the threshold. Subsequently, none of the asynchronous residuals exceed their thresholds, indicating that the fault source can be isolated as d_3 .

flow rate. The sequence of asynchronous measurements for this scenario are:

$$\begin{aligned} t_{k,[In]} &= [0, 0.08, 0.27, 0.61, 0.70, 0.78, 0.79] \text{ hr} \\ t_{k,[M_1]} &= [0, 0.09, 0.09, 0.16, 0.22, 0.52, 0.58, \\ &\quad 0.60, 0.81, 0.93, 0.98] \text{ hr} \\ t_{k,Y} &= [0, 0.02, 0.06, 0.15, 0.38, 0.39, 0.46, 0.48, \\ &\quad 0.55, 0.63, 0.67, 0.68, 0.81, 0.89, 0.99] \text{ hr}. \end{aligned}$$

This simulation study uses the primary control configuration in which Q is the manipulate input, and a fault takes place where $d_3 = 300$ K/s at $t = 0.5$ hr. At this time the synchronous states all move away from the equilibrium point (see [10] for additional figures). Additionally, as asynchronous measurements become available it is observed that the asynchronous states also move away from the equilibrium point after the failure. It is unclear from the state information alone what caused this faulty behavior. However, if the FDI residuals in Figure 7 are examined, the residual associated with T_{g1} , violates its threshold at $t = 0.5003$ hr. The fault is detected upon this threshold violation. However, isolation cannot take place until one new measurement for each asynchronous state becomes available. At $t = 0.6086$ hr all three required asynchronous measurements have become available, and the residuals signal a type I fault, allowing the isolation of the fault to d_3 . The manipulated input for this scenario can be seen in Figure 8.

The final simulation study demonstrates the proposed asynchronous model-based fault-detection and isolation method when a type II fault occurs. The sequence of asynchronous measurements for this scenario are:

$$\begin{aligned} t_{k,[In]} &= [0, 0.34, 0.56, 0.58, 0.6, 0.66, \\ &\quad 0.72, 0.77, 0.80, 0.82] \text{ hr} \\ t_{k,[M_1]} &= [0, 0.21, 0.35, 0.56, 0.57, 0.59, \\ &\quad 0.63, 0.65, 0.70, 0.91, 0.92] \text{ hr} \\ t_{k,Y} &= [0, 0.06, 0.14, 0.22, 0.42, 0.48, 0.54, \\ &\quad 0.59, 0.62, 0.95] \text{ hr}. \end{aligned}$$

This simulation uses the primary control configuration in which Q is the manipulated input. A fault takes place where

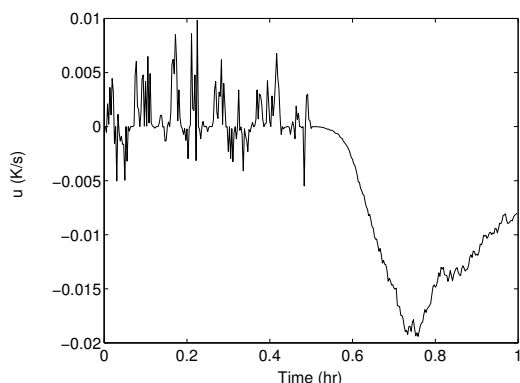


Fig. 8. Manipulated input for the closed-loop system with a fault d_3 at $t = 0.5$ hr.

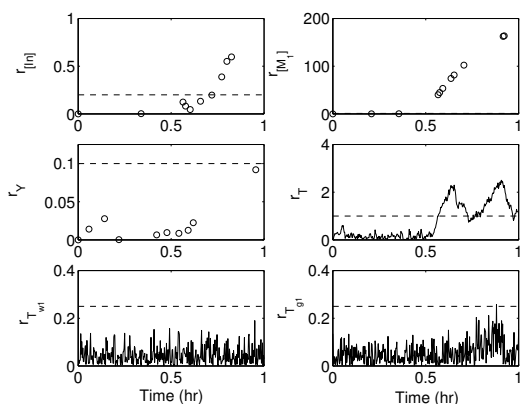


Fig. 9. Fault-detection and isolation residuals for the closed-loop system with a fault d_4 at $t = 0.5$ hr. The fault is detected when residual for $[M_1]$ exceeds the threshold. Subsequently, T and $[n]$ exceed their thresholds. When any asynchronous residual violates the threshold this indicates the fault is in the set of type II faults; d_2 or d_4 .

$d_4 = -0.2$ mol/s at $t = 0.5$ hr representing unexpected monomer consumption. After the failure the synchronous states diverge from their desired values (see [10] for additional figures). Additionally, as asynchronous measurements become available it can be seen that asynchronous states also diverge after the failure. It is unclear from the state information alone what caused this faulty behavior. However, if the FDI residuals in Figure 9 are examined, the residuals $r_{[n]}$, $r_{[M_1]}$, r_T , and $r_{T_{g1}}$ violate their thresholds. The fault is detected upon the first threshold violation ($r_{[M_1]}$ at $t = .05667$ hr). When the residual $r_{[M_1]}$ exceeds the threshold this signals that a type II fault has occurred. When a type II fault occurs it cannot be isolated. As in the second simulation, such a fault can be grouped in the subset of type II faults d_2 or d_4 . At this time, the system operator can utilize the partial isolation to examine the plant and determine the exact source of the failure.

IV. CONCLUSIONS

This work addressed the application of fault-detection and isolation and fault-tolerant control in a polyethylene reactor system where several process measurements were not available synchronously. First, an FDI scheme that employs

model-based techniques was introduced that allowed for the isolation of faults. This scheme employed model-based FDI filters in addition to observers that estimate the fault-free evolution of asynchronously measured states during times when they are unmeasured. Specifically, the proposed FDI scheme provided detection and isolation for a type I fault where the fault entered into the differential equation of only synchronously measured states, and grouping of type II faults where the fault entered into the differential equation of any asynchronously measured state. The detection occurred shortly after a fault took place, and the isolation, limited by the arrival of asynchronous measurements, occurred once all of the asynchronous measurements became available. Once the FDI methodology provided the system supervisor with a fault diagnosis, the supervisor took appropriate action to seamlessly reconfigure the polyethylene reactor system to an alternative control configuration that enforced the desired operation.

REFERENCES

- [1] I. Nimmo, "Adequately address abnormal operations," *Chem. Eng. Prog.*, vol. 91, pp. 36–45, 1995.
- [2] P. Mhaskar, A. Gani, C. McFall, P. D. Christofides, and J. F. Davis, "Fault-tolerant control of nonlinear process systems subject to sensor faults," *AIChE J.*, vol. 53, pp. 654–668, 2007.
- [3] D. Muñoz de la Peña and P. D. Christofides, "Lyapunov-based model predictive control of nonlinear systems subject to data losses," *IEEE Trans. Autom. Contr.*, regular paper in press.
- [4] P. Mhaskar, C. McFall, A. Gani, P. Christofides, and J. Davis, "Isolation and handling of actuator faults in nonlinear systems," *Automatica*, vol. 44, pp. 53–62, 2008.
- [5] K. B. McAuley, D. A. Macdonald, and P. J. McLellan, "Effects of operating conditions on stability of gas-phase polyethylene reactors," *AIChE Journal*, vol. 41, pp. 868–879, 1995.
- [6] G. Walsh, H. Ye, and L. Bushnell, "Stability analysis of networked control systems," *IEEE Transactions on Control Systems Technology*, vol. 10, no. 3, pp. 438–446, 2002.
- [7] D. Nešić and A. R. Teel, "Input-to-state stability of networked control systems," *Automatica*, vol. 40, no. 12, pp. 2121–2128, 2004.
- [8] A. Gani, P. Mhaskar, and P. D. Christofides, "Fault-tolerant control of a polyethylene reactor," *Journal of Process Control*, vol. 17, pp. 439–451, 2007.
- [9] S. A. Dadebo, M. L. Bell, P. J. McLellan, and K. B. McAuley, "Temperature control of industrial gas phase polyethylene reactors," *Journal of Process Control*, vol. 7, pp. 83–95, 1997.
- [10] C. W. McFall, D. Muñoz de la Peña, B. J. Ohran, P. D. Christofides, and J. F. Davis, "Fault detection and isolation for nonlinear process systems using asynchronous measurements," *Industrial & Engineering Chemistry Research*, vol. 47, pp. 10 009–10 019, 2008.
- [11] E. Sontag, "A 'universal' construction of arstein's theorem on nonlinear stabilization," *System and Control Letters*, no. 13, pp. 117–123, 1989.
- [12] N. H. El-Farra and P. D. Christofides, "Integrating robustness, optimality, and constraints in control of nonlinear processes," *Chem. Eng. Sci.*, vol. 56, pp. 1841–1868, 2001.